# Supporting Information

Fe-triazole coordination compound-derived Fe$_2$O$_3$ nanoparticles anchored on Fe-MOF/N-doped carbon nanosheets for efficient electrocatalytic oxygen evolution reaction
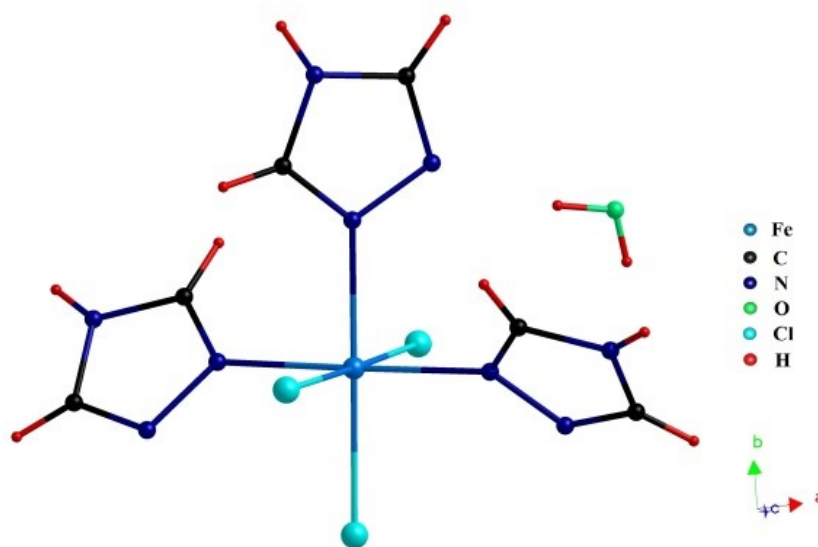
Xing Liu and Yun Gong*

Department of Applied Chemistry, College of Chemistry and Chemical Engineering, Chongqing University, Chongqing 401331, P. R. China. E-mail: gongyun7211@cqu.edu.cn; Tel:+86 023 65678932

(a)
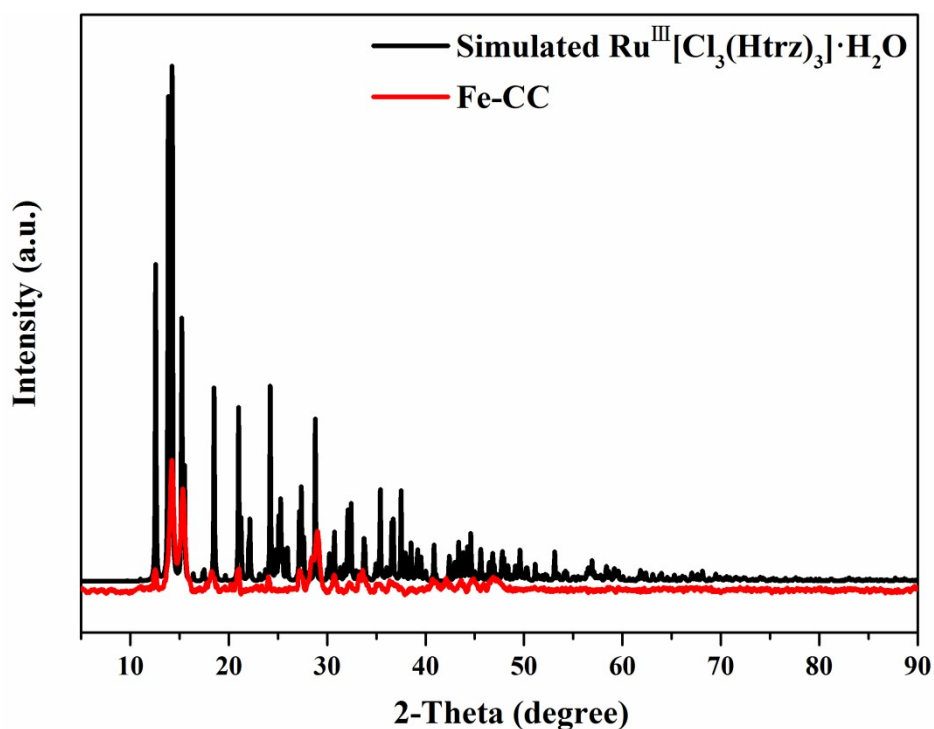
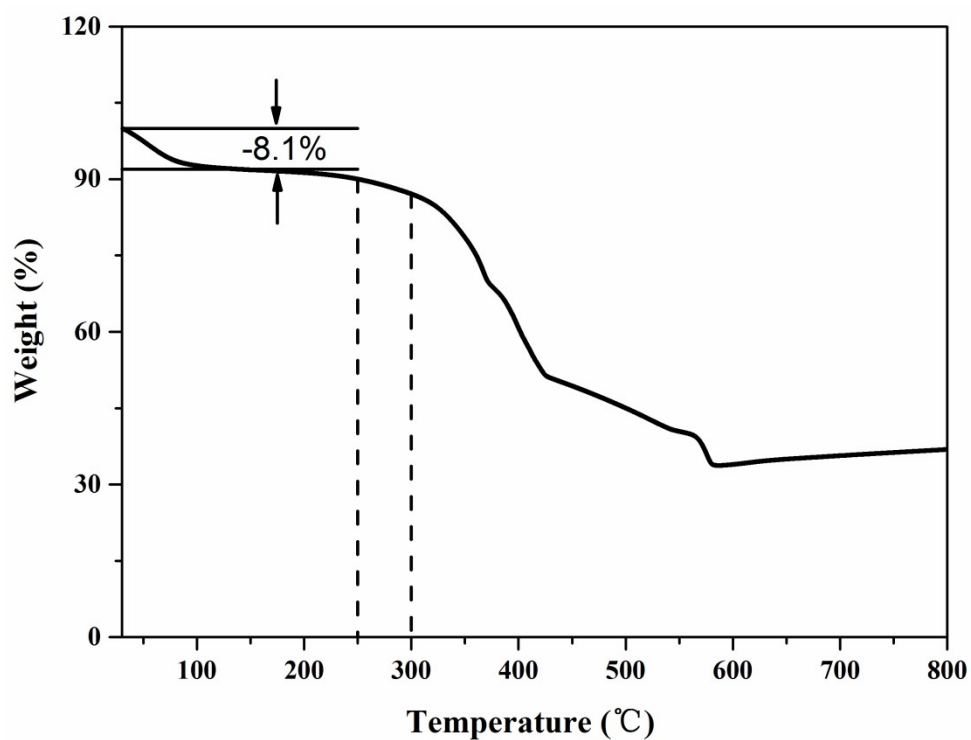**(b)**

(c)

Fig. S1 (**a**) XRD pattern of Fe-CC and the simulated profile of $[Ru^{III}Cl_3(Htrz)_3] \cdot H_2O$;

(**b**) The structure of $[Fe^{III}Cl_3(Htrz)_3] \cdot H_2O$; (**c**) TG curve of Fe-CC; (**d**) XRD of

$Fe_2O_3/NC/Fe$-MOF, Fe_2O_3/NC, the standard profile of Fe_2O_3 and the simulated one of

$[Fe^{II}Cl_2(Htrz)]$.

Syntheses of Fe$_2$O$_3$/NC/Fe-MOF and Fe$_2$O$_3$/NC

The synthesis condition of Fe$_2$O$_3$/NC/Fe-MOF was similar to that of S-doped Fe$_2$O$_3$/NC/Fe-MOF except in the absence of S powder (250°C, 1 h). And the synthesis condition of Fe$_2$O$_3$/NC was similar to that of FeS$_2$/NC except in the absence of S powder (400°C, 1 h). Their XRD patterns are seen in shown in **Fig. S1d**. As shown in **Fig. S2a,** when annealing at 250°C in the absence of S, the XRD pattern of the obtained sample meets well with those of Fe-MOF and Fe$_2$O$_3$, while at the annealing temperature of 400 °Cwithout S, the XRD pattern of the calcined sample perfectly coincides with the standard profile of Fe$_2$O$_3$.

As shown in **Fig. S2(b-d)** and **Fig. S2 (n-p)**, Both Fe$_2$O$_3$/NC/Fe-MOF and Fe$_2$O$_3$/NC are nanoparticles. It is obvious that Fe$_2$O$_3$/NC/Fe-MOF appears to be agglomerated, while Fe$_2$O$_3$/NC is in a more uniform state with higher crystallinity.)
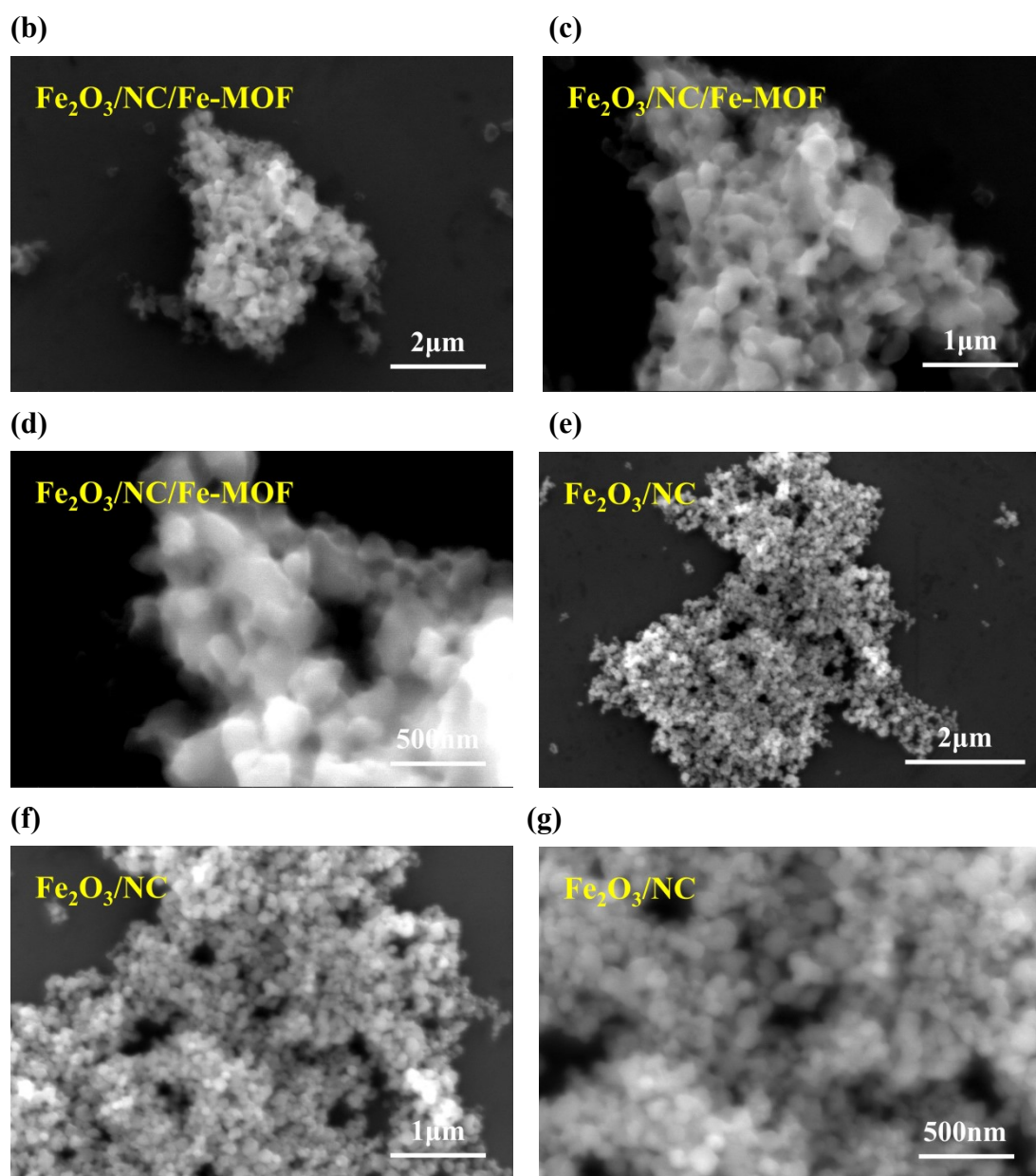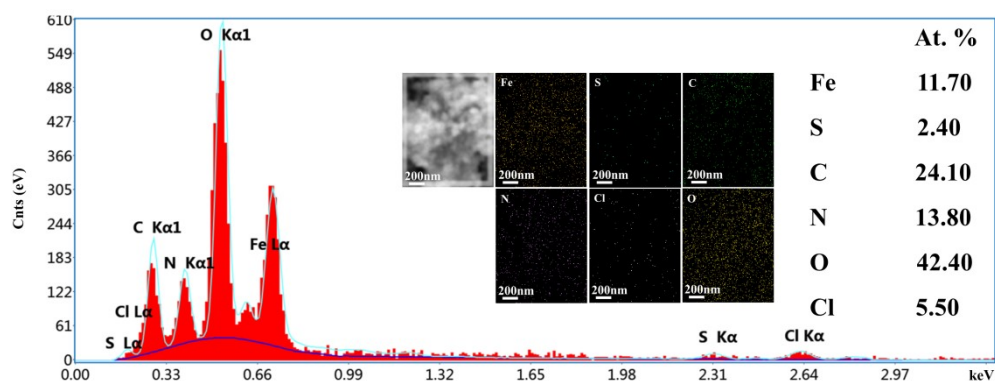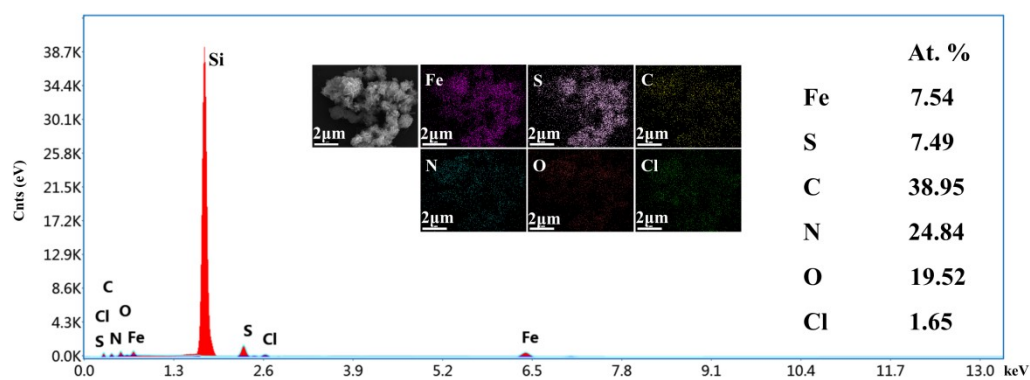
(a)
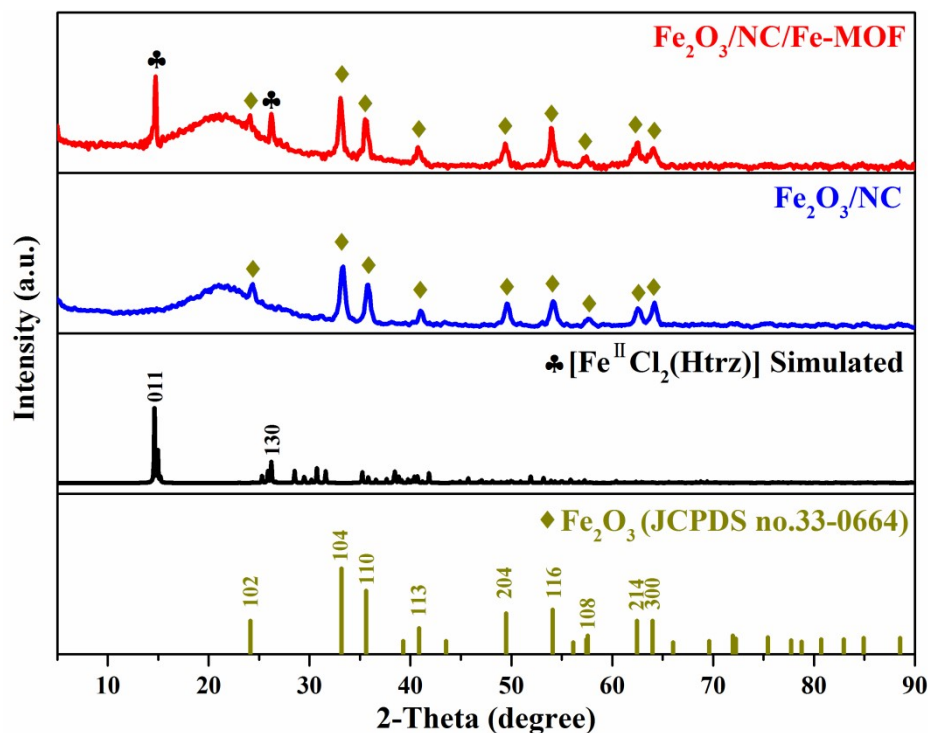
Fig. S2 (**a**) XRD patterns of Fe$_2$O$_3$/NC/Fe-MOF, Fe$_2$O$_3$/NC, the standard profile of Fe$_2$O$_3$ and the simulated one of [Fe^{II}Cl$_2$(Htrz)]; SEM images of (**b-d**) Fe$_2$O$_3$/NC/Fe-MOF and (**e-g**) Fe$_2$O$_3$/NC.

(a)

(b)

(c)
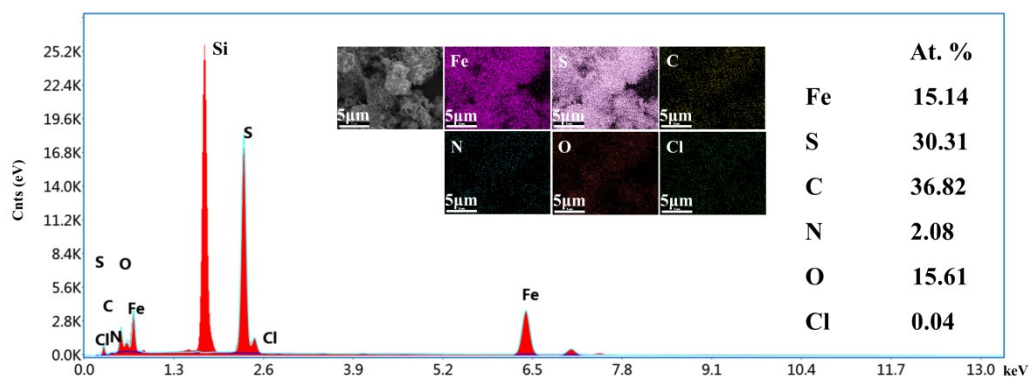
Fig. S3 EDS and elemental mappings for (**a**) S-doped Fe_2O_3/NC/Fe-MOF, (**b**) FeS_2/NC/Fe-MOF and (**c**) FeS_2/NC.
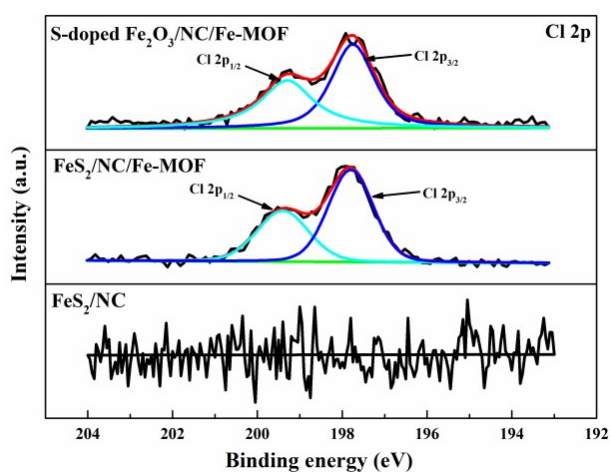
Fig. S4 High-resolution XPS spectra of Cl 2p for the S-doped Fe_2O_3/NC/Fe-MOF, FeS_2/NC/Fe-MOF and FeS_2/NC.

(a) **(b)**

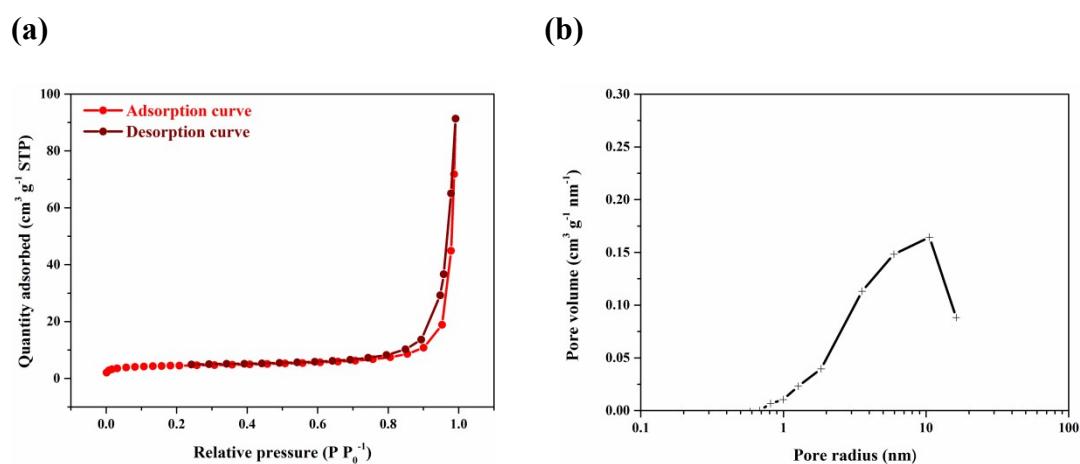**Fig. S5** Nitrogen adsorption/desorption curve and pore size distribution of the S-doped Fe_2O_3/NC/Fe-MOF.

Table S1 Performance comparison of different iron-based catalysts for oxygen evolution reaction.

Catalysts	Overpotential (mV) @ current density (mA cm^{-2})	Tafel slope (mV dec^{-1})	Electrolyte	Reference

This work	**185@10**	**88.4**	**1 M KOH**	
Fe$_2$O$_3$ NPs@NiO NSs/GCE	221@10	53.4	4 M KOH	1
EA-Cu@Fe@Ni/CP	240@10	47	1 M KOH	2
Co$_3$O$_4$/Fe$_2$O$_3$/GCE	310@10	67	1 M KOH	3
Fe$_2$O$_3$/CNT/GCE	410@10	61	1 M KOH	4
P- Fe$_2$O$_3$ -0.45/CP	270@10	72.1	1 M KOH	5
NF/NiSe@Fe$_2$O$_3$/NF	220 @10	36.9	1 M KOH	6
α-Fe$_2$O$_3$/NF	275@10	73.63	1 M KOH	7
Ni$_2$S$_3$/Fe$_2$O$_3$/NC/NF-600	220@100	64.3	1 M KOH	8
MnFeO-NF-0.4/NF	157@10	46	1 M KOH	9
Ni–Fe$_2$O$_3$/GCE	227@10	68	1 M KOH	10
Fe$_2$O$_3$@CuO NTs/CF	398@100	41.07	1 M KOH	11
SS-Fe-0.5/GCE	440@10	68	1 M KOH	12
NiCo/Fe$_3$O$_4$/MOF-74/GCE	238@10	29	1 M KOH	13
Fe$_2$O$_3$/CoO$_x$/CC	315@10	56	1 M KOH	14
CoS$_2$–FeS$_2$/NF	210@10	46	1 M KOH	15
Fe$_3$O$_4$/FeS$_2$-2.5/NF	253@10	48	1 M KOH	16
Fe(ox)(H$_2$O)$_2$/NF-(−1.4)-15	270@40	135	1 M KOH	17
Fe$_3$N-CN/NF	218@10	84	1 M KOH	18
Ni$_{0.7}$Fe$_{0.3}$S$_2$/NF	198@10	56	1 M KOH	19
NiFe(Co$_3$)$_2$--LDH/NF	228@10	37	1 M KOH	20
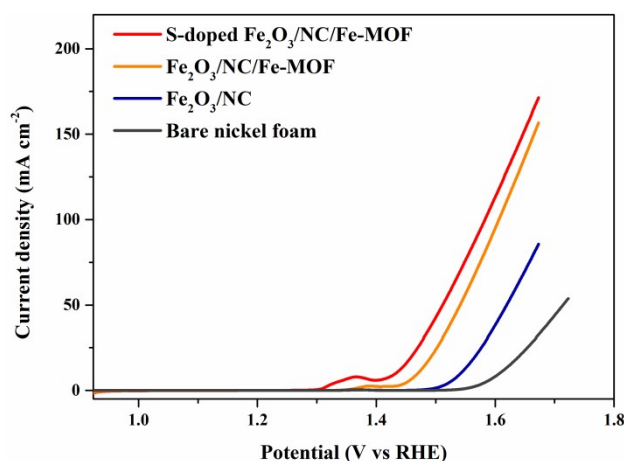
Fig. S6 LSV curves of bare nickel foam, $Fe_2O_3/NC/Fe-MOF$, Fe_2O_3/NC and S-doped $Fe_2O_3/NC/Fe-MOF$.

The LSV curves of $Fe_2O_3/NC/Fe-MOF$ and Fe_2O_3/NC at 2 mV s^{-1} are shown in **Fig. S6**. To achieve 10 mA cm^{-2} of OER current density, the overpotentials (η_{10}) at $Fe_2O_3/NC/Fe-MOF$ and Fe_2O_3/NC are 240 and 312 mV, respectively, which are much larger than that of S-doped $Fe_2O_3/NC/Fe-MOF$ (185 mV). And the OER activity follows the trend: S-doped $Fe_2O_3/NC/Fe-MOF$ > $Fe_2O_3/NC/Fe-MOF$ > Fe_2O_3/NC, indicating the synergistic effect of the components in the S-doped $Fe_2O_3/NC/Fe-MOF$ heterostructure.

Table S2 The parameters in simulated equivalent circuits for the samples

Sample	R_s (Ω cm^{-2})	R_{ct} (Ω cm^{-2})	CPE1	R_{mt} (Ω cm^{-2})	CPE2
S-doped Fe$_2$O$_3$/NC/Fe-MOF	1.057	0.1812	0.4051	0.1126	0.0094
Fe-CC	1.092	0.2244	0.0065	0.1726	0.3399
FeS$_2$/NC/Fe-MOF	1.646	0.2445	0.6274	0.1707	0.0119
FeS$_2$/NC	1.242	0.2128	0.0102	0.1378	0.1093
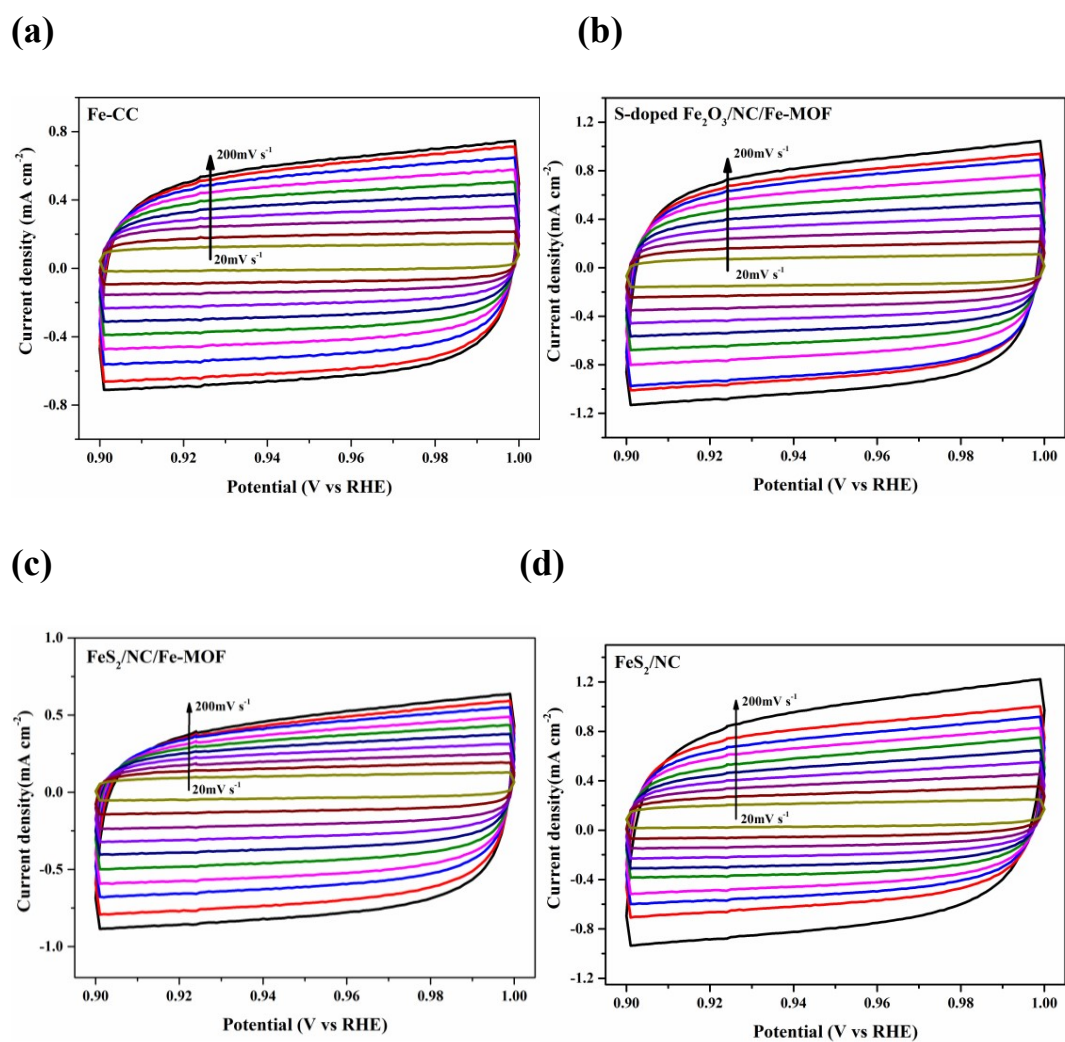
Fig. S7 CV curves of (**a**) Fe-CC, (**b**) S-doped Fe_2O_3/NC/Fe-MOF, (**c**) FeS_2/NC/Fe-MOF and (**d**) FeS_2/NC measured in 1 M KOH solution at different scan rates of 20 to 200 mV s^{-1}.

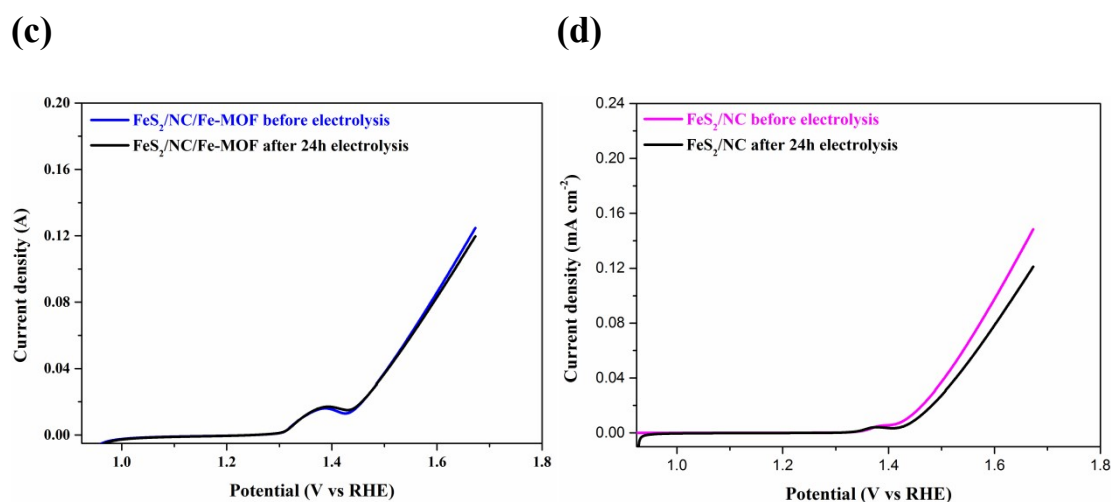**(c)**   **(d)**
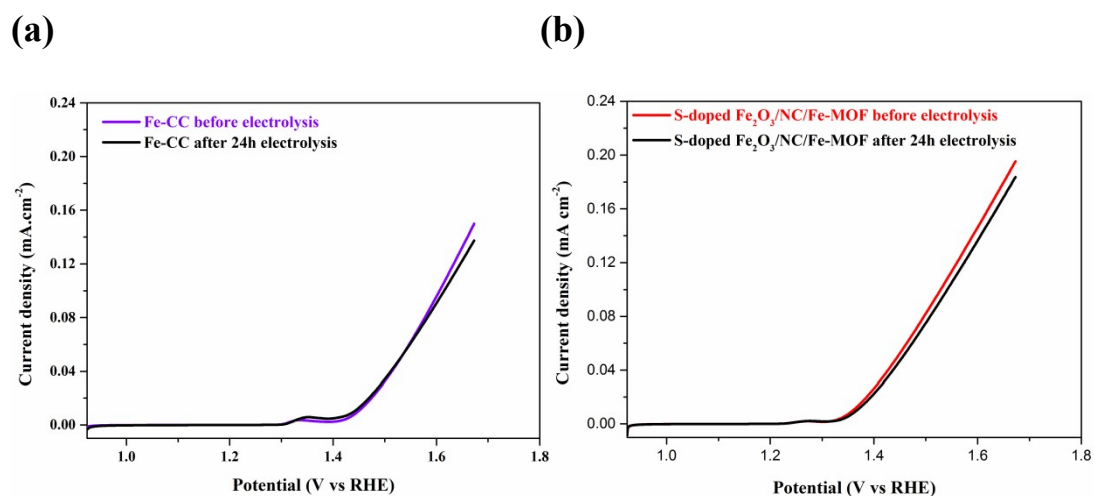
Fig. S8 LSV curves of (**a**) Fe-CC, (**b**) S-doped Fe_2O_3/NC/Fe-MOF, (**c**) FeS_2/NC/Fe-MOF and (**d**) FeS_2/NC before and after 24 h-electrolysis at 2 mV s^{-1}.
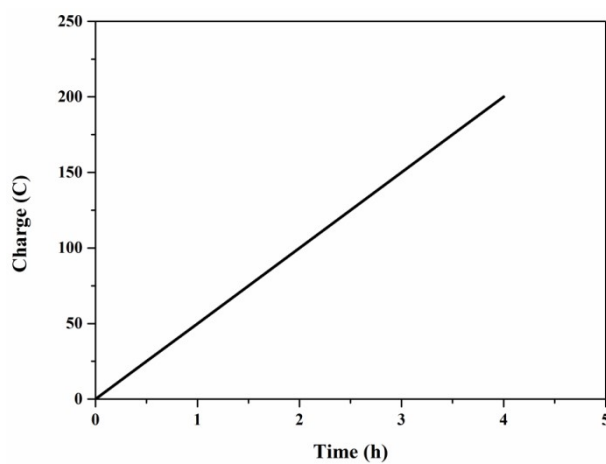

Fig. S9 The plot of charge buildup versus time during 4h-electrolysis at a potential of 1.49 V vs RHE (overpotential $\eta = 0.26$ V).

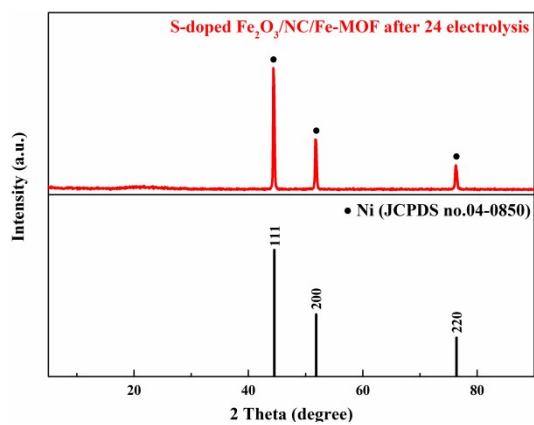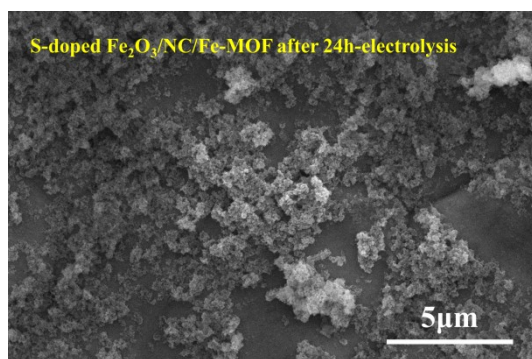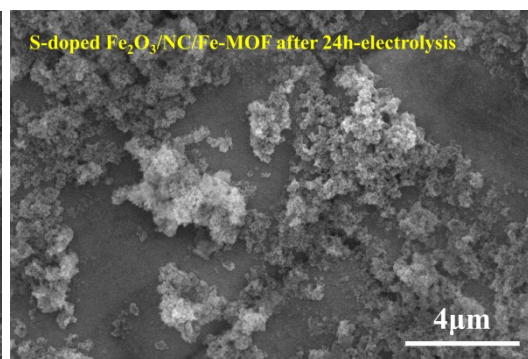**Fig. S10** XRD pattern of S-doped Fe_2O_3/NC/Fe-MOF after 24h-electrolysis and the standard profile of Ni.

(a)   **(b)**
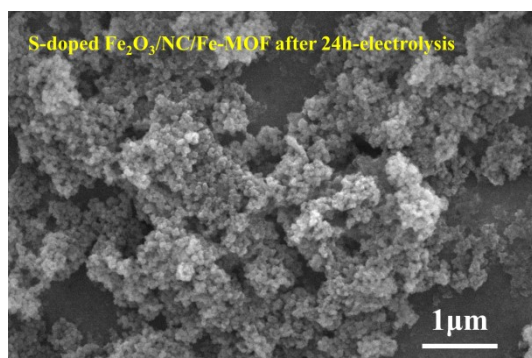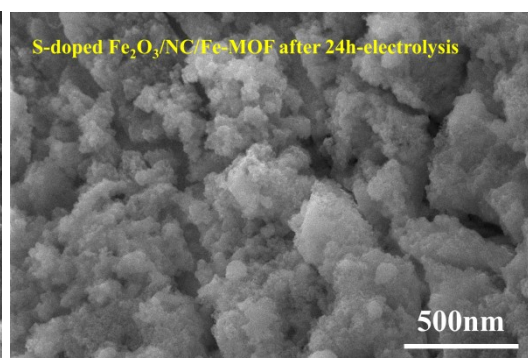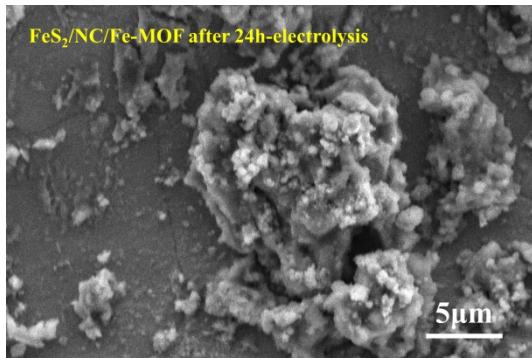

(c)   **(d)**

(e)   **(f)**

(g)
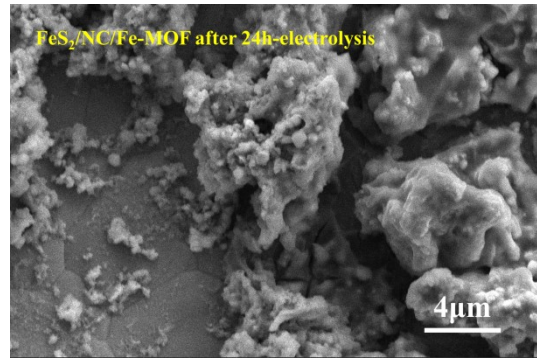
(h)
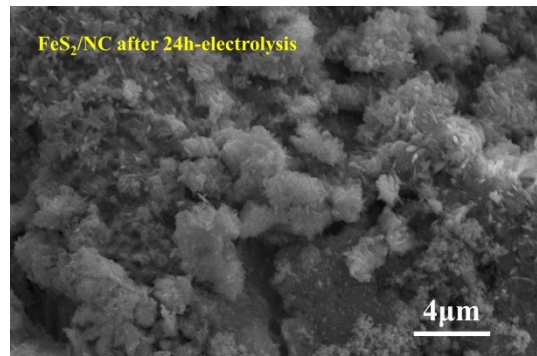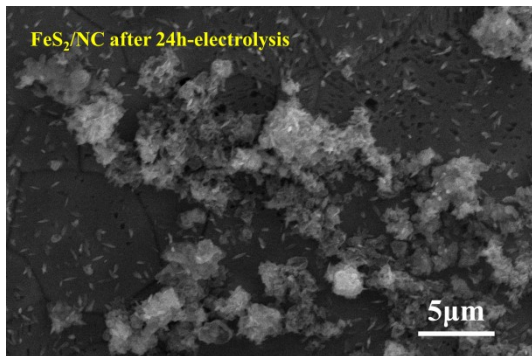
Fig. S11 SEM images of (**a-d**) S-doped Fe_2O_3/NC/Fe-MOF, (**e, f**) FeS_2/NC/Fe-MOF and (**g, h**) FeS_2/NC after 24h-electrolysis.

(a)
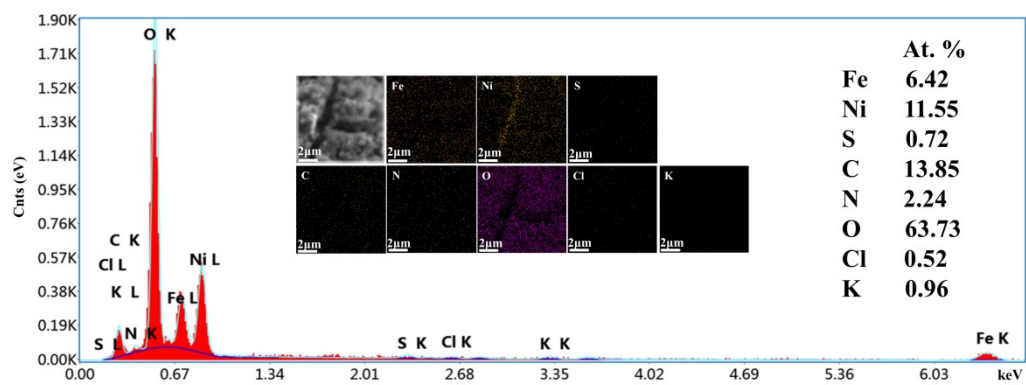
(b)
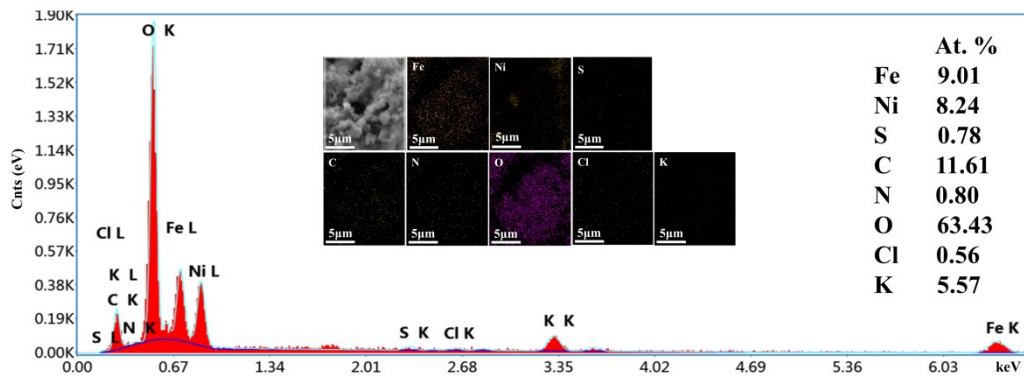
(c)
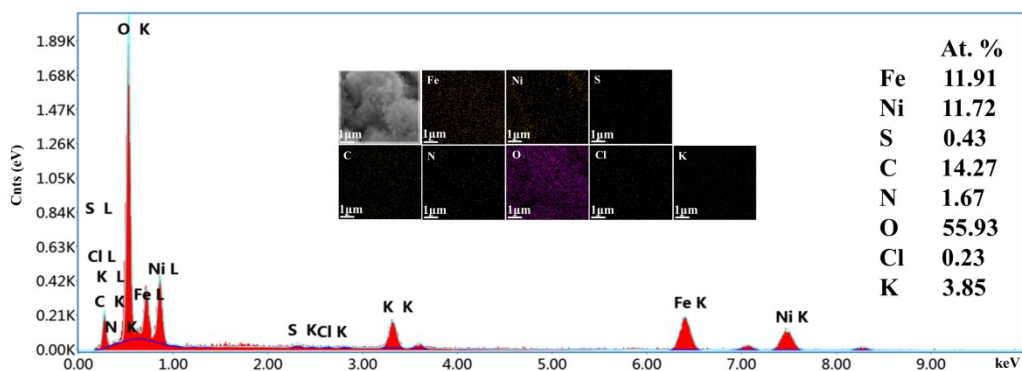
Fig. S12 EDS and elemental mappings for (**a**) S-doped Fe_2O_3/NC/Fe-MOF, (**b**) FeS_2/NC/Fe-MOF and (**c**) FeS_2/NC after 24h-electrolysis.

Table S3 The DFT calculation results for Fe_2O_3 and FeS_2

	Fe-site for Fe_2O_3	Fe-site for FeS_2
$\triangle G_{M-OH*}$ (eV)	0.841	0.859
$\triangle G_{M-O*}$ (eV)	2.043	1.128
$\triangle G_{M-OOH*}$ (eV)	3.835	2.700
$\triangle G_1$ (eV)	1.674	1.692
$\triangle G_2$ (eV)	2.035	1.102
$\triangle G_3$ (eV)	2.625	2.405
$\triangle G_4$ (eV)	1.918	3.053

(a)
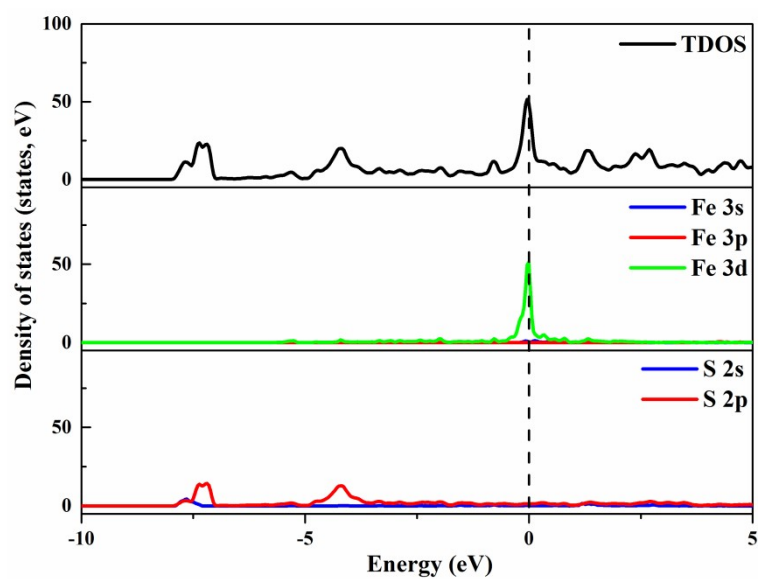
(b)

Fig. S13 TDOS and PDOS for (**a**) FeS$_2$ and (**b**) Fe$_2$O$_3$, in which s, p and d orbitals are denoted in blue, red and green, respectively. The position of the Fermi level is indicated by a black dotted vertical line at 0 eV.

References:

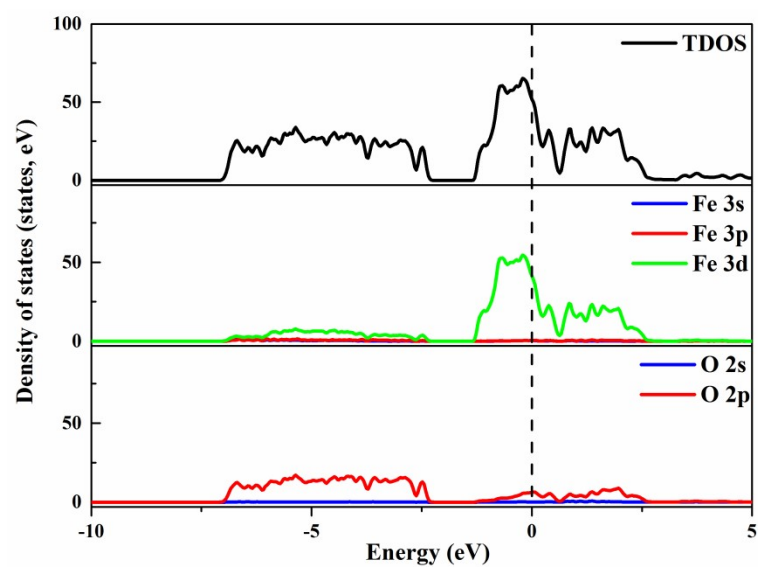1. F. Qiu, J. Shi, M. Guo, S. Chen, J. Xia and Z. H. Lu, *Inorg Chem*, 2021, **60**, 959-966.

2. B. Jiang, Z. Wan, Y. Kang, Y. Guo, J. Henzie, J. Na, H. Li, S. Wang, Y. Bando, Y. Sakka and Y. Yamauchi, *Nano Energy*, 2021, **81**, 105644.

3. X. J. Wei, Y. H. Li, H. R. Peng, D. Gao, Y. Q. Ou, Y. B. Yang, J. R. Hu, Y. H. Zhang and P. Xiao, *Chem Eng J*, 2019, **355**, 336-340.

4. H. A. Bandal, A. R. Jadhav, A. A. Chaugule, W. J. Chung and H. Kim, *Electrochim Acta*, 2016, **222**, 1316-1325.

5. Y. L. Tong, B. Q. Chi, D. L. Qi and W. Q. Zhang, *Rsc Adv*, 2021, **11**, 1233-1240.

6. K. L. Guo, Y. T. Wang, S. Z. Yang, J. F. Huang, Z. H. Zou, H. R. Pan, P. S. Shinde, S. L. Pan, J. E. Huang and C. L. Xu, *Sci Bull*, 2021, **66**, 52-61.

7. Q. Q. Xu, W. Huo, S. S. Li, J. H. Fang, L. Li, B. Y. Zhang, F. Zhang, Y. X. Zhang and S. W. Li, *Appl Surf Sci*, 2020, **533**.

8. S. A. Shah, X. P. Shen, A. H. Yuan, Z. Y. Ji, X. Y. Yue, G. X. Zhu, H. B. Zhou, K. Q. Xu, J. Zhu and Y. Chen, *Appl Surf Sci*, 2020, **527**.

9. J. Luo, W. H. Guo, Q. Zhang, X. H. Wang, L. Shen, H. C. Fu, L. L. Wu, X. H. Chen, H. Q. Luo and N. B. Li, *Nanoscale*, 2020, **12**, 19992-20001.

10. A. Samanta, S. Das and S. Jana, *Acs Sustain Chem Eng*, 2019, **7**, 12117-12124.

11. Y. Gao, N. Zhang, C. R. Wang, F. Zhao and Y. Yu, *Acs Appl Energ Mater*, 2020, **3**, 666-674.

12. C. Q. Li, T. Zhao, S. Y. H. Abdalkarim, Y. H. Wu, M. T. Lu, Y. W. Li, J. K. Gao and J. M. Yao, *Z Anorg Allg Chem*, 2018, **644**, 1103-1107.

13. X. L. Wang, H. Xiao, A. Li, Z. Li, S. J. Liu, Q. H. Zhang, Y. Gong, L. R. Zheng, Y. Q. Zhu, C. Chen, D. S. Wang, Q. Peng, L. Gu, X. D. Han, J. Li and Y. D. Li, *J Am Chem Soc*, 2018, **140**, 15336-15341.

14. S. S. Zhu, L. A. Huang, Z. S. He, K. Wang, J. F. Guo, S. E. Pei, H. B. Shao and J. M. Wang, *J Electroanal Chem*, 2018, **827**, 42-50.

15. W. P. Wang, Y. Xu, J. L. Yao, X. E. Liu, Z. M. Yin and Z. C. Li, *Dalton T*, 2020, **49**, 13352-13358.

16. M. J. Wang, X. Q. Zheng, L. L. Song, X. Feng, Q. Liao, J. Li, L. Li and Z. D. Wei, *J Mater Chem A*, 2020, **8**, 14145-14151.

17. Y. Hai, L. Liu and Y. Gong, *Inorg Chem*, 2021, **60**, 5140-5152.

18. W. Wang, L. Liu, W. C. Leng, L. L. Cui and Y. Gong, *Inorg Chem*, 2021, **60**, 12136-12150.

19. J. H. Yu, G. Z. Cheng and W. Luo, *J Mater Chem A*, 2017, **5**, 15838-15844.

20. S. Liang, B. Wei, M. K. Yuan, Y. Li, X. Ma, Y. Y. Wu and L. L. Xu, *Chemistryselect*, 2020, **5**, 3062-3068.